Composite Particles Gel - Alg – Apatite for Bone Tissue Regeneration

DANIELA PETRE[1], SERGIU CECOLTAN[1], ANDRADA SERAFIM[1], ADRIANA LUNGU[1], DIANA MARIA DRAGUSIN[1], ELIZA GETA STAN[1], CATALIN TUCUREANU[2], EUGENIU VASILE[3], AURORA SALAGEANU[2], MIRCEA ISTODORESCU[4], HORIA IOVU[1], IZABELA CRISTINA STANCU[1]*

[1] University Politehnica of Bucharest, Advanced Polymer Materials Group, 1-7 Ghe Polizu Str., 011061, Bucharest, Romania

[2] Cantacuzino National Institute for Research and Development in Microbiology and Immunology, 103 Spl. Independentei, 050096 Bucharest, Romania

[3] University Politehnica of Bucharest, Faculty of Applied Chemistry and Material Science, Department of Science and Engineering of Oxide Materials and Nanomaterials, 1-7 Gh. Polizu Str., 011061 Bucharest, Romania

[4] S.C. Medical Ortovit S.R.L., 8 Miron Costin Str., 011098, Bucharest, Romania

This paper reports the fabrication of spherical particles developed as bone tissue regenerative biomaterials. Inspired by the extracellular matrix of hard tissues, the particles were generated through the mineral loading of a macromolecular matrix consisting in a bicomponent hydrogel (interpenetrated polymer networks based on gelatin and alginate). The study describes the effects of the peptide-polysaccharide ratio on the morpho-structural features, water affinity, and interaction with MG-63 osteoblast-like cells.

Keywords: spherical particles, biopolymers, hydroxyapatite, bone regeneration

Microparticles based on bovine gelatin (GelB) and alginate (Alg) have been previously investigated by our research group [1, 2] due to their great potential as bone regeneration and bone defects fillers. In this aim we explored methods to generate spherical particles that can be easily used to fill defects of various shapes and sizes. The spherical shape is appealing also due to the possibility to generate inter-particular interconnected pores, needed for bone regeneration and angiogenesis. In addition to such architectural considerations, macromolecular scaffolds based on GelB and Alg are interesting since the two biopolymers are biocompatible and lead to a scaffold mimicking the proteic component of bone extracellular matrix (ECM). Following an ECM-inspired development of the matrix, in this work we report the apatite loading into such organic scaffolds through alternative incubation in Ca^{2+}/PO_4^{3-} baths. The effects of the peptide-polysaccharide ratio on the morpho-structural features, water affinity, and interaction with MG-63 osteoblast-like cells are described.

Experimental part

Materials and methods

All reagents were purchased from Sigma-Aldrich and used without any further purification. Double-distilled water (ddH_2O) prepared with a GFL bidistiller apparatus was used throughout the experiments.

Synthesis of composite hydrogel beads

The synthesis of the composite particles was performed according to the protocol previously described in [1]. Briefly, gelatin B (GelB) aqueous solution (20% wt) was prepared by the graduate dissolution of the protein in double-distilled water (ddH_2O) at 40°C. Sodium alginate (Alg) aqueous solution (4% wt) was prepared by the dissolution of the polysaccharide in ddH_2O at 50°C. GelB-Alg mixtures were obtained by mixing the previously described solutions, under vigorous stirring, at 40°C; different feed ratios have been used, as depicted in table 1. The resulting mixtures were degassed using an ultrasound bath (Elma S 30H, Elmasonic), for 15 min at 40°C. Spherical shaped beads were obtained by extrusion of the homogenous GelB-Alg solution into a $CaCl_2$ solution (1%) under stirring at room temperature, for 30 min. Subsequently, the particles were immersed in a 1% GA aqueous solution in order to crosslink gelatin, for 30 min. The non-reacted GA has been removed by extensive water-extraction, at 40°C. In order to induce the formation of the mineral phase, the so-obtained hydrogel beads were alternatively immersed in Ca^{2+}/PO_4^{3-} solutions, as described by Jaiswal et al [3]. The particles were immersed in 0.5M $CaCl_2$ solution (*p*H 7.4) for 30 min at 37°C, followed by washing with ddH_2O, and then immersed into a 0.3M Na_2HPO_4 solution for 30 min, at 37°C and washed again with ddH_2O. These four steps amount to one cycle of incubation. 6 cycles of incubation were developed for each composition. A Memmert WNE 14 water bath with a shaking device included (speed from 10 to 150 strokes per min, 15 mm stroke - horizontal back/forth movements) was used for the mineralization of the particles. After the final cycle, the particles were immersed in ddH_2O for 2 h, at 37°C and dried. For simplicity, the resulted composites will be further are denoted as Mi, where M states for mineralization, while i represents the ratio GelB:Alg (table 1).

Characterization

Effect of composition over mineral loading

In order to determine the amount of mineral phase formed within the beads, samples of each composition were dried at 37°C, weighted dry and subsequently immersed in 0.2M HCl solution, known for its ability to dissolve the mineral [4–6]. After 24 h, the samples were removed from the incubation media, dried and weighted again. The amount of mineral was estimated as the mass

Sample	GelB:Alg, [wt%]
M5	5:1
M10	10:1
M25	25:1

Table 1
REACTION MIXTURES USED TO PREPARE THE HYDROGELS Mi

* email: izabela.cristina.stancu@gmail.com; Tel.: +40 21 402 2718

lost during acid incubation and it was calculated as percentage of the initial mass of the dried composite, before acid treatment.

Attenuated Total Reflectance - Fourier-Transform Infrared Spectrometry (ATR -FTIR)

The FTIR analysis was performed in order to assess the presence of mineral phase after the Ca^{2+}/PO_4^{3-} incubation. The analysis was performed on the surface of the samples and on the powder obtained after cryogenic grinding in liquid nitrogen. A JASCO 4200 spectrometer equipped with a Specac Golden Gate attenuated total reflectance device (ATR) was used, by accumulating 100 spectra in the 4000–600 cm^{-1} wavenumber interval.

Scanning electron microscopy (SEM)

Morpho-structural analysis of the mineralized samples was performed through SEM, using, both oven-dried (at 37°C) and lyophilized samples. The lyophilization of the samples was performed at -50°C using a Martin-Christ freeze-dryer, and the resulting materials will be further denoted MiL. The analysis was performed using a QUANTA INSPECT F SEM device equipped with a field emission gun (FEG) with a resolution of 1.2 nm, on the surface and in cross-sections, using samples coated with a thin gold layer (coating for 40 s).

Water affinity

Water affinity was assessed gravimetrically. Briefly, samples were immersed in ddH_2O at 37°C. At predetermined intervals, the samples were removed from the incubation media, blotted with filter paper to absorb the excess of water on the surface, and then weighed again. This procedure was repeated until equilibrium was reached. The swelling rate (SR) was calculated as follows:

$$SR(\%) = \frac{m_t - m_0}{m_0} \cdot 100 \quad (1)$$

where m_t and m_o represents the mass of the microspheres in the swelling state, at time t, while m_o represents the initial mass, before incubation in ddH_2O, respectively.

The equilibrium water content (EWC) was calculated using equation (2):

$$EWC(\%) = \frac{m_{max} - m_0}{m_{max}} \cdot 100 \quad (2)$$

where m_{max} is the weight of the microspheres after equilibrium was reached and m_0 is the initial mass of the sample. All data points are the mean ± standard deviation of three separate measurements.

Biocompatibility assessment

In order to perform cell culture tests, films with selected composition were used. Mineralized and non-mineralized materials were seeded with MG-63 cells to explore the effect of mineral phase on cell behavior. The synthesis protocol of the films was similar with the one described above, with the soul difference that the polymer mixture was not dripped into $CaCl_2$ solution, but physically crosslinked at 4°C and subsequently immersed in 1% $CaCl_2$ aqueous solution, followed by immersion in 1% GA solution. Disks were punched out of the gels using a punch closely fitting the well diameter of 24-well tissue culture plates and, subsequently, mineralized following the protocol described above. Mi disks were sterilized by overnight incubation in 70% ethyl alcohol and washed in sterile phosphate buffered saline (PBS). Prior to transfer to 24-well tissue culture plates, disks were equilibrated in culture media (DMEM, 100 U/mL penicillin-streptomycin, no serum supplementation). Non-mineralized films (NMi) were used as control.

Cell culture

MG-63 human osteosarcoma cell-line (ECACC) were cultured in Dulbecco's Modified Eagle Medium (DMEM) (Sigma-Aldrich) supplemented with 10% fetal bovine serum (FBS) (GIBCO) and 100 U/mL penicillin-streptomycin (Lonza). Cells were detached by trypsination, seeded at 10^5 cells/well for 24h or $2.5x10^4$ cells/well for 7 days, and incubated at 37°C in a humidified atmosphere with 5% CO_2.

Microscopy

Following incubation, non-adherent cells were removed by gently washing twice with PBS, and attached cells were stained 5 min with 2µg/mL acridine orange (AO) and 4ug/mL propidium iodide (PI) in PBS at 37°C and fixed for 10 min in 2% paraformaldehyde. Mi disks were removed from the wells, mounted face down on regular microscopy slides and imaged on a Nikon TE2000U microscope using a 5MP cooled CCD camera and a 20x long working distance objective. For each field, separate grayscale images (16bit TIFF) were taken using epifluorescence filter blocks (AO - λEx 455-495nm, λEm 500-545nm; PI - ëEx 510-560nm, λEm 590-600nm) and DIC.

Results and discussions

GelB-Alg scaffolds were obtained as elastic beads in fully hydrated state. Their incubation in alternate Ca^{2+}/PO_4^{3-} baths lead to a evident mineral loading, as visible in figure 1. The stability of the mineral phase to the organic substrate after several washing cycles and subsequent drying was confirmed.

FTIR analysis

The FTIR-ATR spectra (fig. 2) successfully confirmed the presence of a newly formed mineral phase, following alternate incubation. Nano-hydroxyapatite (n-HA) was used as control sample and its spectrum was characterized by a sharp peak at 3571 cm^{-1} corresponding to the stretching vibration of hydroxyl group and by the peaks at 600 and 1020 cm^{-1} corresponding to stretching vibrations of P–O bonds in the phosphate network of hydroxyapatite, as

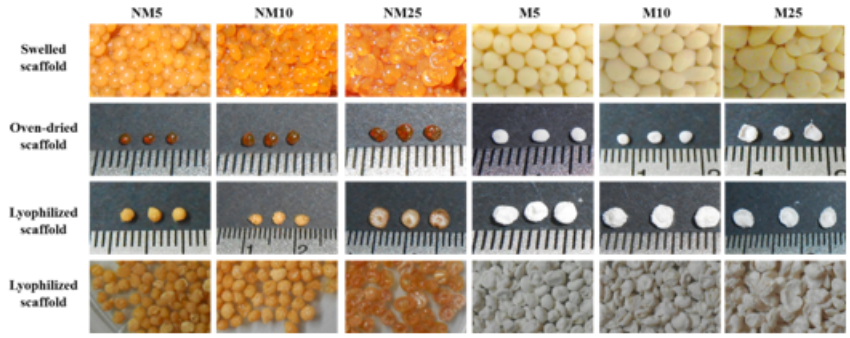

Fig. 1. Non-mineralized (NMi) and mineralized (Mi) compositions (digital photos)

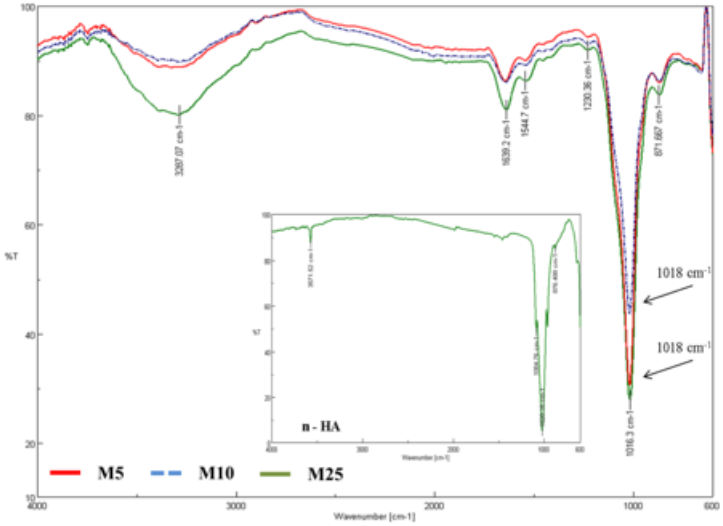

Fig. 2. FT-IR spectra of Mi samples (inset - spectrum of n-HA)

previously reported [7]. The spectra of the composite materials obtained through mineralization using the "alternate soaking" method presented typical phosphate vibrations in the 1000-1100 cm^{-1} range. Also, it was noticed that the peak of PO_4^{3-} groups at 1018 cm^{-1} in M10 sample showed a shift to 1016 cm^{-1} for the M25 sample and the intensity got stronger with increasing Alg.

Effect of hydrogel composition over mineral loading

The mineral dissolution through immersion of the composites in HCl solution confirmed an influence of the composition on the mineral phase formation. Increasing the amount of protein in the hydrogel scaffold leads to a decrease of the dissolved mineral content in the Mi samples. Accordingly, the amount of Ca-P mineral was estimated to be 63.55% for M5, 52.89% for M10 and only 48.7% for the M25 sample.

Morphology investigation

Morphologic information regarding the hybrid polymer-apatite beads were obtained through SEM for both oven-dried and freeze dried samples. The images of the samples dried at 37°C are illustrated figure 3. The alternate incubation in Ca^{2+}/PO_4^{3-} solutions led to the formation of thick compact layers of brittle mineral onto the surface of all samples. Apatite crystals were also embedded in the hydrogel matrix, as visible in the cross-section images of the samples; individual nanometric crystals, with morphology typical to nano-apatite, were more abundant in the sample containing the lowest Alg amount, M25. It can be observed that with increasing the peptide content, the morphology of the Mi samples gradually changed from plate-like (M5) to needle-like (M25) crystals, suggesting that a lower content of Alg enhanced crystallinity. In a similar study, Rajkumar et al [8] also reported that the mineral phase growth is relatively increased when a lower amount of Alg is present in the polymer matrix. Such a result confirmed that the organic matrix of the composites has a great influence on the crystallinity and morphology of the mineral.

The SEM images recorded for the freeze dried samples are depicted in figure 4. As expected, freeze drying the fully hydrated samples lead to porous scaffolds. The SEM images registered on the surface of the MiL series (fig. 4, top row) did not identify pores, probably due to the high amount of mineral which, after drying formed a compact layer on the surface, closing the inner pores. However, images recorded in cross-section (fig. 4, bottom row)

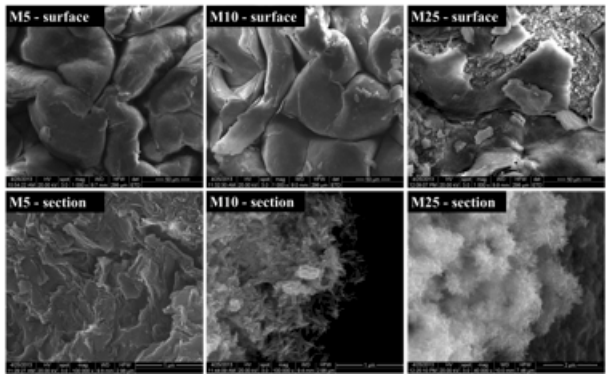

Fig. 3. SEM images for the Mi series: top row – surface; bottom row – cross-section

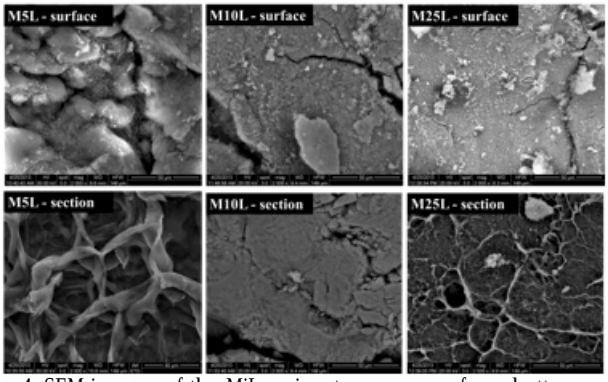

Fig. 4. SEM images of the MiL series: top row – surface; bottom row – cross-section

clearly revealed porous structures. Mineral deposits are visible, as in the case of the Mi series, both on the surface, as well as inside the samples, confirming the composite nature of the materials. Morphological differences were noticed for the different compositions, as visible in figure 4.

Water affinity of the composite hydrogels

The water uptake capacity of a hydrogel is influenced by factors including the hydrophilicity of the constituents, crosslinking degree and chemical composition. A variation in the chemical composition of the network can effectively control the swelling of the hydrophilic macromolecular matrices [9]. Swelling ratios of Mi composites were calculated using eq. 1.

The results (fig. 5) revealed that all materials swelled relatively fast, reaching their maximum swelling degree (MSD) in less than one hour. MSD values ranged between 196.55 ± 2.47 (M25) and 171.6 ± 1.6 (M5). Also, EWC was similar for all compositions, with calculated values around

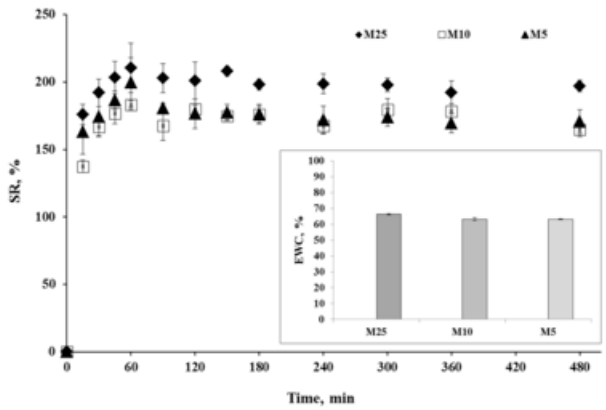

Fig.5. Swelling behavior as a function of time for Mi composite materials, inset – EWC, %

65%. However, the results indicated that decreasing Alg content was associated with a slight increase of EWC. The obtained results are in agreement with the results previously reported by Saarai and Hanna [10, 11].

Biocompatibility test

Adhesion, spreading and proliferation of MG-63 cells was assessed using M5 disks. Since all the composites presented a compact mineral shell, the Ca/P incubation procedure was adjusted and the cellular response to the obtained composites was investigated. Briefly, NM5 disks were immersed for 6 h and 12 h, respectively, in Ca followed by P solutions resulting in M5-6 and M5-12 scaffolds. Cells that were either weakly adherent or growing in suspension were removed by pipetting, while remaining cells were fixed and stained with AO and PI prior to microscopic examination, in order to allow both observation of cell morphology and visualization of late apoptotic and necrotic cells(PI permeable). As sample preparation for microscopy involved a series of washing steps it probably also resulted in displacement of non-viable cells, as PI positive cells were only observed in the non-adherent cell fraction and not on the M5 films. Consequently, only representative AO fluorescence photomicrographs are shown in figure 6. Following 24h incubation a small number of adhering cells could be observed on the un-mineralized NM5 films with some of them showing an elongated, spindle shaped morphology (fig. 6, A). Adhesion seemed inhibited by mineral deposition on both M5-6 and M5-12 samples, as both fewer cells and more rounded cellular morphology were observed on these substrates (fig. 6, B and C). Intriguingly, for 7 days cultures no adhering cells were observed on the NM5 films across all imaged fields. Toxicity can be ruled out as a significant number of cells were found growing in large non-adherent clumps in the same wells. It is possible that the lower seeding density used for the 7 days experiment in combination with the low percentage of adhering cells resulted in sparse cell distribution across the substrate and limited cell-cell contacts, thus disfavoring proliferation on the simple NM5 films. It is also possible that the lengthy incubation at 37°C lead to degradation of surface exposed gelatin and consequent detachment of cells as alginate alone is insufficient to promote adhesion [12].

After 7 days in culture significant numbers of MG-63 cells were found adherent to both mineralized M5-6 and M5-12 films. However, there was a significant difference in morphology of cells grown on the two substrates (fig. 6, E and F). Cells on the M5-12 films were polygonal and flattened, showing morphology suggestive of stronger adherence while on M5-12 most cells were spindle shaped, thus having limited contact with the substrate, and seemed to proliferate in multi-stratified clusters where cell-cell adhesion is dominant. The increased number of cells observed at 7 days and not 24h cultures on the M5-6 and M5-12 films suggests that cell adhesion and spreading on these substrates may require previous adsorption of either serum components or cell-derived proteins to the mineralized polymers.

In conclusion, it appears that mineralization promote MG-63 cell adhesion and spreading on M5 substrates, but also that different mineralization procedures affect the way cells interact with the scaffold. Further biochemical and molecular studies will be performed to assess the influence of these substrates on the expression of phenotypic markers for osteoblast differentiation.

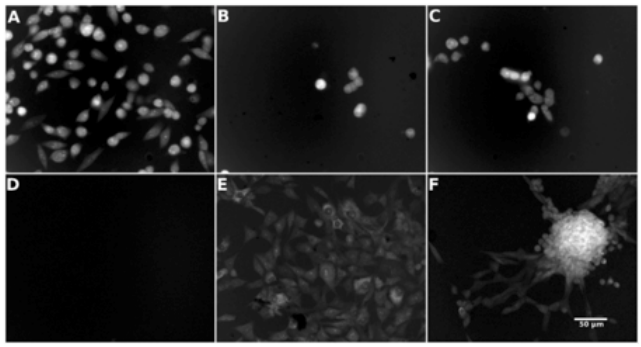

Fig. 6. MG-63 cultured on control (NM5) and mineralized (M5) films; images represent cells cultured for 24h (A, B, C) and 7 days (D, E, F) on NM5 (A, D), M5-6 (B, E) and M5-12 (C, F)

Conclusions

The present work refers to the synthesis and characterization of spherical particles consisting in composite materials based on two biopolymers (GelB and Alg) and apatite, developed for bone tissue regeneration and repair. The fabrication of the materials combines the initial generation of an interpenetrated polymer network (IPN), followed by the loading with mineral phase using the alternate incubation of the hydrogels in Ca/P baths. It was established that the composition of the polymeric matrix influences not only the water affinity of the scaffolds, but also the amount and morphology of the mineral phase as well as the cellular response. Thus, decreasing the GelB:Alg ratio leads to more stable particles, with higher content of mineral and lower water affinity. The biological tests showed that all compositions have potential for bone tissue regeneration.

Acknowledgement:The work has been funded by the Sectorial Operational Programme Human Resources Development 2007-2013 of the Ministry of European Funds through the Financial Agreement POSDRU/159/1.5/S/132397. Also the authors would like to acknowledge the financial support from the project 183/2012, Bioactive Injectable Macroporous Biomaterials for Bone Regeneration.

References

1. PETRE D.G., SERAFIM A., LUNGU A., VASILE E., CRISTESCU I., ISTODORESCU M., Key Eng. Mater., **614**, pp. 26–30, 2014.
2. CECOLTAN S., PETRE D. G., STAN E. G., VASILE E., CIOFLAN H. E., ISTODORESCU M., CRISTESCU I., MARINESCU R., LAPTOIU D., STANCU I. C., Key Eng. Mater., **638**, pp. 20–26, 2015.
3. JAISWAL A. K., KADAM S. S., SONI V. P., BELLARE J. R., Appl. Surf. Sci., **268**, pp. 477–488, 2013.
4. STANCU I. C., FILMON R., CINCU C., MARCULESCU B., ZAHARIA C., TOURMEN Y., BASLE M., and CHAPPARD D., Biomaterials, **25**, no. 2, pp. 205–213, Jan. 2004.
5. HANKERMEYER C. R., OHASHI K. L., DELANEY D. C., ROSS J., CONSTANTZ B. R., Biomaterials, **23**, no. 3, pp. 743–750, Feb. 2002.
6. DEMIRBA^{a} A., ABALI Y., MERT E., Resour. Conserv. Recycl., **26**, no. 3–4, pp. 251–258, Jun. 1999.
7. MOBINI S., JAVADPOUR J., HOSSEINALIPOUR M., GHAZI-KHANSARI M., KHAVANDI A., REZAIE H. R., Adv. Appl. Ceram., **107**, no. 1, pp. 4–8, 2008.
8. RAJKUMAR M., MEENAKSHISUNDARAM N., RAJENDRAN V., Mater. Charact., **62**, no. 5, pp. 469–479, May 2011.
9. ROY A., BAJPAI J., BAJPAI A. K., Indian J. Chem. Technol., **16**, no. 5, pp. 388–395, 2009.
10. HANNA P. A., GAD S., GHONAIM H. M., GHORAB M. M., Br. J. Pharm. Res., **3**, no. 4, pp. 597–616, 201AD.
11. SAARAI A., KASPARKOVA V., SEDLACEK T., SAHA P., J. Mech. Behav. Biomed. Mater., **18**, pp. 152–166, Feb. 2013.
12. WANG L., SHELTON R. M., COOPER P. R., LAWSON M., TRIFFITT J. T., BARRALET J. E., Biomaterials, **24**, no. 20, pp. 3475–3481, Sep. 2003

Manuscript received: 6. 08. 2015